EAST EUROPEAN JOURNAL OF PHYSICS. 4. 506-511 (2025)
DOI:10.26565/2312-4334-2025-4-51 ISSN 2312-4334

LOCAL VARIATION OF SCATTERING LIGHT INTENSITY IN MANGANESE ION IMPLANTED SILICON SINGLE CRYSTALS

E.U. Arzikulov[1,2,3]*, F.A. Salaxitdinov[1], Wang Yujin[2], Shaowei Lu[3], Teng Liu[3], Zhisheng Nong[3], M.D. Toshboyev[1]

[1]*Samarkand State University named after Sharof Rashidov, 140104, 15, University Blvd., Samarkand, Republic of Uzbekistan*
[2]*State Key Laboratory of Precision Welding & Joining of Materials and Structures, School of Material Science and Engineering, Harbin Institute of Technology Yikuang Street, Nangang District, Harbin 150001, China*
[3]*School of Material Science and Engineering, Shenyang Aerospace University, 37 Daoyi South Avenue, Shenyang, China*
**Corresponding Author e-mail: eshkuvata@gmail.com*
Received September 2, 2025; revised October 22, 2025; accepted November 4, 2025

This article presents the results of experimental studies of local changes in the scattered light intensity and surface morphology in Mn implanted single-crystal silicon samples with electron conductivity and [100] crystalline orientation. The manganese ion energy, implantation dose, and phosphorus concentration in substrate were 40 keV, $5\cdot10^{15}\div1\cdot10^{17}$ ion/cm^2, and ~ $9.3\cdot10^{14}$ cm^{-3}, respectively. Atomic force microscopy (AFM) and Raman spectroscopy, using the backscattering geometry of surface-scattered light, were applied to analyze the surface morphology before and after implantation. AFM micrographs of the surface show characteristic nanometer-sized roughnesses, the shape and size of which strongly depend on the implantation dose. These nanoscale objects are not present on the non-implanted substrate surface. In the Raman spectra of the samples not subjected to implantation, the main Lorentz-type peak is always observed, which is characteristic of single-crystal silicon and centered at 520.0±1.0 cm^{-1}, corresponding to the phonon wave vector. Several peaks are observed in the Raman spectra of manganese ion-implanted silicon samples (184, 291, 373, 468, 659, 798, and 804 cm^{-1}), presumably associated with the formation of radiation defects and nanoscale objects on the surface of single-crystal silicon during ion implantation with the participation of silicon, manganese, phosphorus, and other impurity atoms. These structural defects in the silicon crystal lattice at the surface and near-surface caused by manganese ion bombardment lead to the excitation of new vibrational modes not observed in the initial silicon. These modes are manifested in Raman scattering spectra.
Key words: *Local intensity; Ion implantation; Raman scattering; Silicon; Nanoscale objects; Wave vector*
PACS: 33.20. Fb; 42.68. Mj; 61.72. Tt

INTRODUCTION

Recently, there has been significant interest in the development and study of silicon nanocrystals and their nanostructures, particularly their optical, electronic, and other properties. This is due to their possible implementation in different devices, such as high-performance solar cells, non-volatile memory devices, biomedical devices and sensors, anode materials for lithium-ion batteries, active materials for thermoelectric devices, and efficient photon sources. Ion implantation (II) is an advanced technique for forming nanoscale structures in the surface and near-surface regions of semiconductors, enabling the design of nanoelectronic devices. The properties of nanoelectronic devices depend largely on the size, shape, and concentration of nanoscale structures in the surface and near-surface layers of the semiconductor substrate.

The study of nanoscale structure formation involving impurities in solids, especially semiconductors such as silicon, is of significant scientific and practical interest. This interest stems from two factors: (1) these structures significantly alter the physicochemical properties of the material, often imparting unique characteristics, and (2) these materials enable the development of highly sensitive sensors for various external stimuli [1]. Impurities are introduced into semiconductors primarily through diffusion, ion implantation, or doping during growth [2]. Impurities from transition metals create deep energy levels in the silicon band gap, significantly altering its generation-recombination properties. These deep levels modify the properties of silicon typically doped with shallow-level impurities, enabling new phenomena with potential applications in modern electronics. Transition metal impurities are typically introduced into the silicon volume via high-temperature diffusion. However, diffusion doping has a significant drawback: the limited solubility of transition metal impurities in silicon restricts the practical use of diffusion-doped materials. Ion implantation overcomes this limitation [3]. It allows the introduction of impurities into the semiconductor at concentrations far exceeding their maximum solubility [4]. By introducing sufficient impurities via ion implantation, self-organized nanoscale structures can form, involving impurities and structural defects. This significantly modifies the properties of the original material, imparting tailored characteristics that underscore the relevance of this work. This article presents an experimental study of local variations in scattered light intensity on the surface of Mn implanted monocrystalline silicon samples containing nanoscale structures. It also examines their surface morphology, geometric dimensions, and shapes.

Cite as: E.U. Arzikulov, F.A. Salaxitdinov, W. Yujin, S. Lu, T. Liu, Z. Nong, M.D. Toshboyev, East Eur. J. Phys. 4, 506 (2025), https://doi.org/10.26565/2312-4334-2025-4-51

MATERIALS AND METHODS

Bilaterally polished single-crystal silicon plates with electron conductivity and crystallographic orientation [100] were chosen as the substrate material for the ion-implantation process. The electron concentration in the substrate was approximately ~ $9.3 \cdot 10^{14}$ cm^{-3}. Implantation of manganese ions with an energy of 40 keV was performed on the ILU-3 linear ion accelerator at room temperature. The implantation dose varied in the $5{,}0 \cdot 10^{15} \div 1{,}0 \cdot 10^{17}$ ion/cm^2 range.

In modern conditions, highly sensitive microscopic, X-ray, spectroscopic, and other methods are mainly used to detect nanocrystals and nanostructures in solids or low-dimensional systems. In particular, the Raman (Micro Raman or μ-Raman) and AFM methods have recently become one of the generally accepted tools for studying bulk and low-dimensional materials, especially single-crystal silicon and nanostructures based on it [5-9].

In this studies was used AFM and Raman spectroscopy to characterize the surface morphology and dimensions of nanoscale structures. It is known that both of these methods are highly accurate and informative tools for studying the formation of nanoscale structures in various materials. In addition, Raman spectroscopy provides valuable information on local atomic ordering and phonon modes [10, 11]. For the effective practical application of ion-implanted materials, it is necessary to know their physical properties in damaged surface layers: phase state, concentration of free charges, etc. Recent studies by the authors of [10] have shown that Raman scattering is a powerful tool for determining the physical characteristics of ion-implanted silicon layers. Our experiments recorded Raman spectra using a Renishaw InVia micro-Raman spectrometer at room temperature in the wavenumber range of 50 to 1000 cm^{-1}. The spectra were recorded in the backscattering geometry with a spectral resolution better than 2.0 cm^{-1}. The incident radiation was not polarized, and the optical recording scheme also did not include polarizing filters. A Cobalt CW DPSS solid-state laser with a wavelength of 532 nm and a nominal power of 50 mW was used as an excitation source. The exciting laser beam was focused on the sample surface using a 100× objective. A similar procedure was used to collect scattered light. The obtained spectra were processed using the Origin Pro 18 software package.

To study the surface morphology of monocrystalline silicon samples, a multifunctional AFM Core 300 was used in the static force mode. AFM Core 300 is a device with a unique set of capabilities for studying various properties of surfaces (and chips) of materials with high (up to atomic) resolution. The operating principle of this device is based on scanning the surface with solid-state sharp probes (needles) in the process of their mutual movement according to specified algorithms. A distinctive feature of the AFM, along with high resolution, is the ability to obtain a pseudo-three-dimensional image of the surface with visualization of quantitative data on its electrical, magnetic, topographic and other characteristics.

RESULTS AND DISCUSSION

The results of the experiments on Raman spectroscopy are shown in Figure 1. The measurements were carried out at three different points on surface of initial and manganese ion-implanted monocrystalline silicon samples.

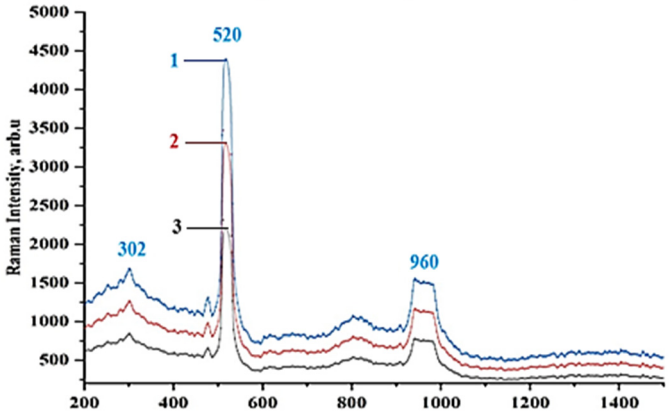

Figure 1. Raman spectra for the original bulk sample (1) with thickness of 3 mm, (2) and (3) with thicknesses of 500 and 200 μm, as well as for a plate of single-crystal silicon doped with phosphorus

As shown in Figure 1, the Raman spectrum of the original (non-implanted) silicon samples contains the main peak with a wave number of 520 cm^{-1} and accompanying peaks (satellites) at frequencies of 301 cm^{-1} and in the range of 900-971 cm^{-1}. It is known that Raman spectroscopy is especially sensitive to the surface condition and thickness of the samples. To clarify the effect of thickness on the appearance of the Raman spectra and the intensity of the peaks in them, we measured the dependence of the Raman spectra on the thickness of the semiconductor substrate. Our experimental results showed that increasing the thickness of non-implanted samples from 200 μm to 3 mm leads to an approximately 50% decrease in the intensity of the main Raman peak at 520 cm^{-1}, while its spectral position remains unchanged. The measured full width at half maximum (FWHM) of this peak for the 3-mm-thick sample was 3.9 cm^{-1}, and for the 200-μm-thick sample, it was 4.2 cm^{-1}. Analysis of these results suggests that sample thickness significantly influences the Raman spectra. This is due to the penetration depth of the exciting light, the energy of which E_0=1.95 eV is greater than the band gap of single-crystal silicon equal to E_g=1.12 eV, and energy scattering in the volume. Secondary radiation

occurs only in a thin near-surface layer with a thickness of several microns. Thus, thicker samples result in greater attenuation of secondary order scattered light, reducing its intensity, as observed in our experiments. This means that the analysis of the Raman spectra provides information only on the near-surface layer. Thus, it can be argued that the observed features of the Raman spectra, such as local intensity, position, and shape of the phonon band, etc., provide valuable information about nanoscale objects, their composition and structure of both original and ion-implanted single-crystal samples and thin silicon wafers.

The Raman spectra shown in Figure 1 (a), (b) clearly show the main Lorentzian peak characteristic of crystalline silicon (c-Si). This peak is centered at approximately 520.0±1.0 cm^{-1} and corresponds to the phonon wave vector. The recorded Raman spectral parameters, such as peak position and intensity, are consistent with data reported in the [12, 13]. The long-range translational symmetry of crystalline silicon potentially allows the appearance of additional peaks in the range of 100÷1100 cm^{-1}. Although their intensity is considerably weaker than that of the main first-order longitudinal-transverse optical (LTO) phonon peak [14]. Additionally, these spectra (Figure 1a, b) contain a broad band in the range of 925÷985 cm^{-1}. A similar broad band in the range of 900÷1100 cm^{-1} was previously reported in the spectra of nanocrystalline silicon [11, 15], attributed to the scattering of multiple transverse optical (2TO) phonons and their overtone states.

Figure 2 shows the Raman spectra of Mn implanted silicon samples. These spectra, acquired at three distinct surface locations, reveal several additional bands of varying intensities. The number and intensity of these bands vary significantly with implantation dose.

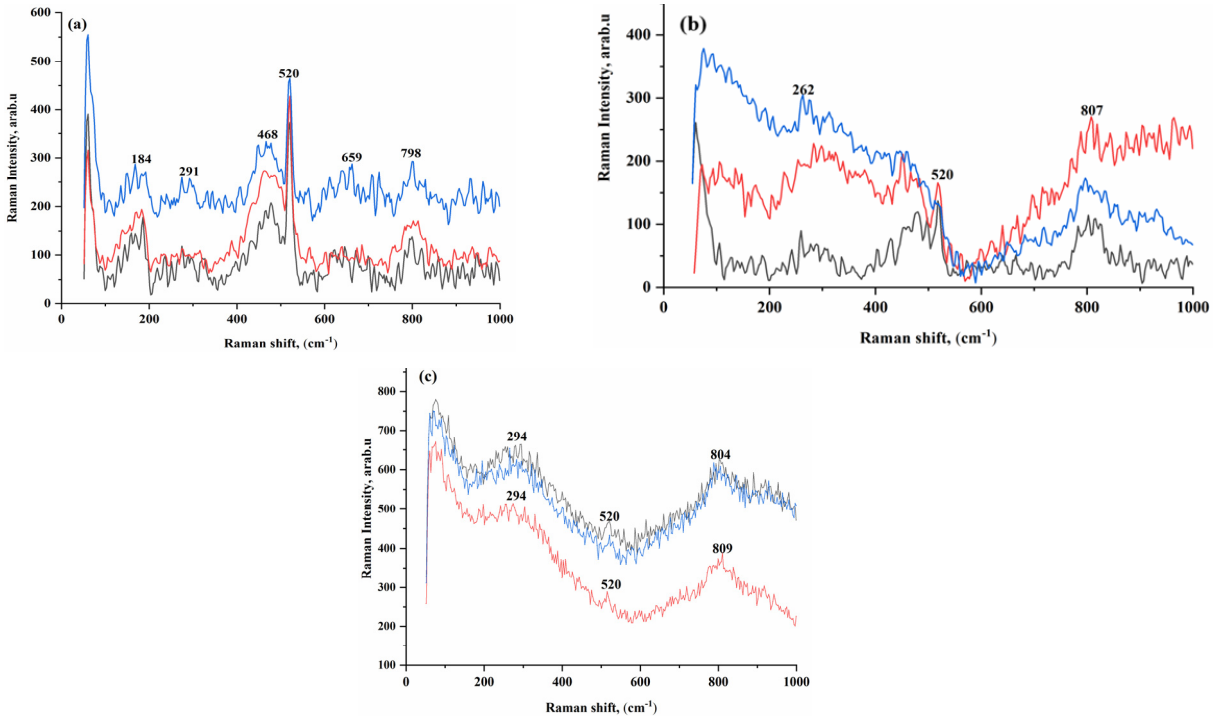

Figure 2. Change in the local intensity of the Raman spectra of ion-implanted silicon samples measured at three different points on the surface depending on the implantation dose, ion/cm^2: (a) – $5{,}0\cdot10^{15}$, (b) – $5{,}0\cdot10^{16}$, (c) – $1{,}0\cdot10^{17}$; ion energy 40 keV; T = 300 K

Thus, for example, at relatively low (Figure 2, (a)) doses equal to $5{,}0\cdot10^{15}$ ion/cm^2 in the Raman spectra, a sufficiently intense main peak of the quasi-Lorentz shape, characteristic of crystalline silicon (c-Si), is still clearly expressed and it retains its position relative to the center located at approximately a frequency of 520.0±1.0 cm^{-1} and still corresponds to the phonon wave vector. It should be noted that at low implantation doses, only a decrease in the intensity of the Raman peaks is observed, associated with both fundamental and higher scattering orders, which probably contributed to the formation of point defects. In addition, in the Raman spectra, a number of satellites are observed located relative to the central peak corresponding to 520.0 cm^{-1} both toward low (184, 291, 468 cm^{-1}) and toward high frequencies (659, 798 cm^{-1}), which can probably be associated with the formation of nanosized defect structures of the silicon crystal lattice that arose under the influence of the II process. As shown in Figure 2(b), increasing the implantation dose significantly alters the Raman spectral profile and the intensities of its peaks.

Starting with a dose of $5{,}0\cdot10^{16}$ ion/cm^2, although the position of the central peak remains unchanged, its intensity decreases approximately 2,6 times and new satellites appear located at frequencies of 262 and 807 cm^{-1} with very low intensity, indicating a violation of the crystal lattice, and correlating with the one-phonon density of states. Further increase of the implantation dose to $1{,}0\cdot10^{17}$ ion/cm^2 (Figure 2, (c)) leads to the virtual disappearance of the central peak (its intensity is at the noise level), the low-frequency satellite shifts toward high frequencies (294 cm^{-1}), and the high-frequency satellite is in the frequency range of 804÷807 cm^{-1}.

Our previous studies [16] investigated the generation mechanisms of nanoscale structures in Mn implanted single-crystal silicon. Using Raman spectroscopy and AFM, we obtained detailed information on both initial and ion-implanted samples. According to [16], increasing implantation dose results in the formation of various phase states in the near-surface layers of silicon. Their characteristics, such as the position in the spectrum and intensity, depend on the implantation dose and the position of the laser radiation incidence point on the sample, which is confirmed by our results. The experimental results on the dose dependence of Raman scattering in silicon samples implanted with manganese ions can be explained as follows. At relatively low implantation doses, the damage to the silicon crystal lattice is insignificant, which causes the existence of a peak with a frequency of 520.0 cm^{-1} corresponding to single-crystal silicon, and a decrease in its intensity can be associated with partial destruction of the crystal lattice. It can be stated that the intensity of the peak with a frequency of 520.0 cm^{-1} corresponding to single-crystal silicon can be considered as an indicator of the substrate crystallinity. The lower its intensity, the stronger the destruction of its crystallinity. The appearance of low- and high-frequency satellites in the Raman spectra can be associated with nanoscale structural defects, as well as defects involving manganese atoms (ions) and other impurity atoms. This assumption is also supported by the change in the position and intensity of such satellites depending on the implantation dose. With an increase in the implantation dose, the substrate surface begins to transform into an amorphous state, which in turn is characterized by a random arrangement of matrix atoms (silicon), manganese ions and other foreign atoms. As was said above, the Raman spectroscopy method is sensitive to the environment of the matrix (substrate) atoms. The presence and arrangement of impurities around silicon atoms notably alter the Raman spectral profile, including the position of the high-frequency satellite peak (Figure 2(c)). We have suggested that the detected peaks arise from radiation-induced defects in the crystal structure and nanoscale structures formed primarily from silicon, manganese, phosphorus, and other impurities on the surface of single-crystal silicon during ion irradiation. To test this hypothesis, we conducted additional studies of the surface morphology of the samples before and after implantation using the AFM method. To analyze the surface morphology of single-crystal silicon samples before and after implantation, an AFM from Nano Surf, Core AFM 300, was used. The obtained images of the surface topology of the manganese-implanted single-crystal silicon samples we studied showed that they contain roughness with dimensions of the order of nanometers (Figure 3).

In addition, the obtained AFM images revealed the presence of various types of nanosized objects on the sample surface, presumably bound by silicon and phosphorus atoms, with embedded manganese ions and a number of other impurity atoms, or the formation of nanosized structural radiation defects during II. To analyze changes in the surface morphology of the samples before and after ion beam treatment, its surface was measured using AFM in the electrostatic force mode. Figure 3 shows AFM images demonstrating the surface relief features of nanostructured silicon samples.

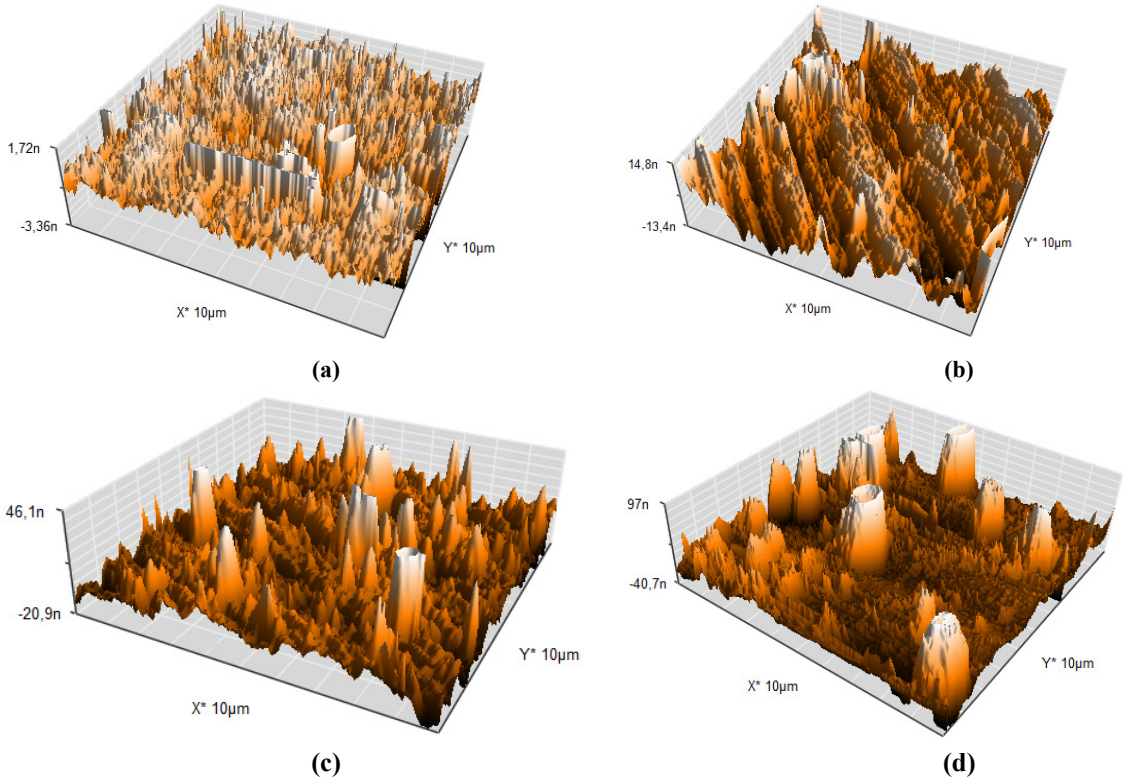

Figure 3. AFM images of the surface of single-crystal silicon before (a) and after manganese ion implantation (40 keV, 300 K) at doses of: (b) $5{,}0\cdot10^{15}$ ion/cm^2, (c) $5{,}0\cdot10^{16}$ ion/cm^2, (d) $1{,}0\cdot10^{17}$ ion/cm^2.

Analysis of Figure 3 demonstrates that an increase in the implantation dose dramatically transforms the surface topography, making it noticeably rougher. The surface roughness of the original, non-implanted samples is relatively

smoother (Figure 3(a)) than that of those implanted with doses: $5{,}0\cdot10^{15}$ ion/cm^2 (Figure 3(b)); $5{,}0\cdot10^{16}$ ion/cm^2 (Figure 3(d)) and $1{,}0\cdot10^{17}$ ion/cm^2 (Figure 3(c)). In parallel with this, the dimensions of the nanostructures formed on the surface increase as the dose of implanted ions increases. In addition, the results of AFM studies confirm the presence of silicon nanowires or nanocrystals on the substrate surface. The transverse dimensions of these formations increase significantly depending on the concentration of implanted ions: from approximately 9 nm at a dose of $5{,}0\cdot10^{15}$ ion/cm^2 (Figure. 3(b)) to ~ 200 nm at a dose of $1{,}0\cdot10^{17}$ ion/cm^2 (Figure. 3(d)). It is known that II causes the formation of various radiation defects on the surface and near it, which significantly changes the properties of the material. The nature, type, structure and composition of these defects change significantly with increasing energy and implantation dose. Examples of such defects in silicon include vacancies associated with oxygen or phosphorus [17-20]. According to [21], ion implantation leads to the appearance of structural defects. The appearance of new peaks in the Raman spectra of ion-implanted samples is probably due to these radiation-induced structural defects. External defects may also be present, such as impurity elements (non-silicon atoms) that may occupy interstitial or nodal positions (substitutional impurities). As a result of the activation of these impurities under various external influences, they may lead to the formation of more complexes, such as impurity-vacancy pairs, etc. [22].

CONCLUSIONS

In the Raman spectra of the studied samples of manganese ion implanted single-crystal silicon with an energy of 40 keV and with different implantation doses, new peaks were recorded at frequencies of 184, 291, 373, 468, 659, 798 and 804 cm^{-1}, which are located relative to the central peak corresponding to the frequency of 520.0 cm^{-1} both toward low (184, 291, 373, 468 cm^{-1}) and toward high frequencies (659, 798, 804 cm^{-1}), which can probably be associated with the formation of nanoscale defect structures of the silicon crystal lattice that arose under the influence of the ion irradiation process.

Local variations in scattered light intensity and the Raman phonon band's position and shape provide important information insights into the structure and composition of nanoscale features in ion-implanted single-crystal silicon samples.

Analysis of the first-order Raman spectral shift indicates that thickness-dependent differences are likely due to variations in light penetration depth in the near-surface region and energy dissipation within the sample.

The occurrence of secondary peaks in the Raman spectra is associated with the formation of nanoscale objects consisting mainly of matrix atoms (silicon), phosphorus, manganese ions and other impurity atoms, as well as radiation-induced structural defects arising under the influence of the ion implantation process.

Analysis of AFM images of Mn implanted single-crystal silicon surfaces revealed silicon nanowires or nanocrystals, with their sizes increasing with implantation dose. The transverse dimensions of these structures increase significantly with ion dose, from approximately 9 nm at 5.0×10^{15} ions/cm^2 to ~200 nm at 1.0×10^{17} ions/cm^2. Thus, ion implantation induces significant structural changes in silicon, forming defects and nanoscale structures that can be characterized using Raman spectroscopy and AFM.

ORCID

Eshkuvat U. Arzikulov, https://orcid.org/0000-0001-9179-3402; **Wang Yujin**, https://orcid.org/0000-0002-8710-1108

REFERENCES

[1] P. Jagadeesh, S.M. Rangappa, and S. Siengchin, Adv. Ind. and Eng. Poly. Res. **7**, 122 (2024). https://doi.org/10.1016/j.aiepr.2023.03.002
[2] S.K. Jha, and M. Kumar, International Open-Access, Double-Blind, Peer-Reviewed, Refereed, Multidisciplinary Online Journal (IJARSCT), **4**, 685 (2024). https://doi.org/10.48175/IJARSCT-19475
[3] Y.G. Abov, F.S. Dzheparov, N.O. Elyutin, D.V. Lvov, and A.N. Tyulyusov, Physics of Atomic Nuclei, **79**, 617 (2016). https://doi.org/10.1134/S1063778816040037
[4] S. Cho, and B.-G. Park, in: *Doping: Properties, Mechanisms and Applications,* edited by Lixin Yu (Nanchang University, PR China, 2013), https://novapublishers.com/wp-content/uploads/2019/08/978-1-62618-097-0_ch4
[5] C. Meiera, S. Lu, V.G. Kravets, H. Nienhaus, A. Lorke, and H. Wiggers, Physica E, **32**, 155 (2006). http://dx.doi.org/10.1016/j.physe.2005.12.030
[6] Z. Guoliang, L. Pan, Z. Chengxi, G. Xinran, D. Ronglu, and Y. Liangbao, Anal. Chem. **97**, 5612 (2025). https://doi.org/10.1021/acs.analchem. 4c0629
[7] M.I. Suib, A.F.A. Rahim, L.N. Ismail, K.Y. Lee, and A.R.M. Radzol, in: *2024 IEEE-EMBS Conference on Biomedical Engineering and Sciences (IECBES) Proceedings*, (Penang, Malaysia, 2024), pp. 483-488. https://doi.org/10.1109/IECBES61011.2024. 10990872
[8] Y. Duan, J.F. Kong, and W.Z. Shen, J. Raman Spec. **43**, 756 (2012). https://doi.org/10.1002/jrs.3094.
[9] M. Khorasaninejad, J. Walia, and S. Saini, Nanotechnology **23**, 275706 (2012). https://doi.org/10.1088/0957-4484/23/27/275706
[10] E. Smith, and G. Dent, *Modern Raman spectroscopy: a practical approach,* 2nd ed, (Wiley, Hoboken, NJ, 2019), pp. 23-67. https://doi.org/10.1002/0470011831.ch5
[11] M. Cardona, *Light Scattering in Solids*. (Springer, Berlin, Heidelberg, 1982), pp.147–248.
[12] H. Richter, Z.P. Wang, and L. Ley, Solid State Communications, **39**, 625 (1981). https://doi.org/10.1016/0038-1098(81)90337-9
[13] F. Minoru, K. Yoshihiko, H. Shinji, and Y. Keiichi, Phys. Rev. B, **54**, R8373(R) (1996). https://doi.org/10.1103/PhysRevB.54.R8373
[14] I. Iatsunskyi, G. Nowaczyk, S. Jurga, V. Fedorenko, M. Pavlenko, and V. Smyntyna, Int. J. for Light and Elec. Opt. **126**, 1650 (2016).

[15] Á. Fernández-Galiana, O. Bibikova, S.V. Pedersen, and M.M. Stevens, Adv. Mater. **36**, 2210807 (2024). https://doi.org/10.1002/adma. 202210807
[16] E.U. Arzikulov, F.A. Salakhitdinov, F. Kholmurodov, and M.D. Tashboev, J. of Phys.: Conference Series, **2573**, (2023). https://doi.org/10.1088/1742-6596/2573/1/012015
[17] V. Pelenitsyn, and P. Korotaev, Comput. Mat. Sci. **207**, 111273 (2022). https://doi.org/10.1016/j.commatsci.2022.111273
[18] M.D. McCluskey, and A. Janotti, Appl. Phys. **127**, 190401 (2020). https://doi.org/10.1063/5.0012677
[19] M.D. McCluskey, and E.E. Haller, *Dopants and Defects in Semiconductors*, 2nd ed. (CRC Press, 2018).
[20] F. Tuomisto, *Characterization and Control of Defects in Semiconductors*, (IET, 2019).
[21] L.P. Avakyants, V.S. Gorelik, and E.D. Obraztsova, J. of Molecular Structure, **219**, 141 (1990).
[22] F. Cristiano, PhD. Dissertation, Université Paul Sabatier - Toulouse III, 2013.

ЛОКАЛЬНА ВАРІАЦІЯ ІНТЕНСИВНОСТІ РОЗСІЯНОГО СВІТЛА В МОНОКРИСТАЛАХ КРЕМНІЮ З ІМПЛАНТАЦІЄЮ ІОНІВ МАРГАНЦЮ

Е.У. Арзікулов[1,2,3], Ф.А. Салаксітдінов[1], Ван Юйцзінь[2], Шаовей Лу[3], Тен Лю[3], Чжишен Нун[3], М.Д. Тошбоєв[1]
[1]Самаркандський державний університет імені Шарофа Рашидова,
140104, бульвар Університету, 15, Самарканд, Республіка Узбекистан
[2]Державна ключова лабораторія прецизійного зварювання та з'єднання матеріалів і конструкцій, Школа матеріалознавства та інженерії, Харбінський технологічний інститут, вул. Ікуан, район Нанган, Харбін 150001, Китай
[3]Школа матеріалознавства та інженерії, Шеньянський аерокосмічний університет, проспект Даої Саут, 37, Шеньян, Китай

У цій статті представлені результати експериментальних досліджень локальних змін інтенсивності розсіяного світла та морфології поверхні у зразках монокристалічного кремнію з електронною провідністю та кристалічною орієнтацією [100], імплантованих Mn. Енергія іонів марганцю, доза імплантації та концентрація фосфору в підкладці становили 40 кеВ, $5\cdot10^{15}\div1\cdot10^{17}$ іонів/см^2 та ~$9{,}3\cdot10^{14}$ см$^{-3}$ відповідно. Для аналізу морфології поверхні до та після імплантації було застосовано атомно-силову мікроскопію (АСМ) та раманівську спектроскопію з використанням геометрії зворотного розсіювання поверхнево розсіяного світла. АСМ-мікрофотографії поверхні показують характерні нанометрові шорсткості, форма та розмір яких сильно залежать від дози імплантації. Ці нанорозмірні об'єкти відсутні на поверхні неімплантованої підкладки. У раманівських спектрах зразків, що не піддавалися імплантації, завжди спостерігається основний пік лоренцовського типу, характерний для монокристалічного кремнію та зосереджений на 520.0±1.0 см$^{-1}$, що відповідає фононному хвильовому вектору. У раманівських спектрах зразків кремнію, імплантованого іонами марганцю, спостерігається кілька піків (184, 291, 373, 468, 659, 798 та 804 см$^{-1}$), ймовірно пов'язаних з утворенням радіаційних дефектів та нанорозмірних об'єктів на поверхні монокристалічного кремнію під час іонної імплантації за участю атомів кремнію, марганцю, фосфору та інших домішок. Ці структурні дефекти кристалічної решітки кремнію на поверхні та поблизу поверхні, спричинені бомбардуванням іонами марганцю, призводять до збудження нових коливальних мод, які не спостерігаються у вихідному кремнії. Ці моди проявляються у спектрах комбінаційного розсіювання.

Ключові слова: *локальна інтенсивність; іонна імплантація; комбінаційне розсіювання; кремній; нанорозмірні об'єкти; хвильовий вектор*